Mesoporous Structures from Supramolecular Assembly of in situ Generated ZnS Nanoparticles

Rohit Kumar Rana,[†] Lizhi Zhang,[‡] Jimmy C. Yu,[‡] Yitzhak Mastai,[§] and Aharon Gedanken*,[†]

Department of Chemistry, Bar-Ilan University, Ramat-Gan 52900, Israel, Department of Chemistry, The Chinese University of Hong Kong, Shatin, New Territories, Hong Kong, China, and Max Planck Institute of Colloids and Interfaces, Golm, Germany

Received March 2, 2003. In Final Form: April 25, 2003

A stable mesoporous network formed by nanoparticles of ZnS was achieved by an ultrasound-mediated fabrication method. The ZnS nanoparticles were generated in situ during the sonication, and dodecylamine was used as the structure-directing agent. All the synthesized materials were characterized using X-ray diffraction, high-resolution transmission electron microscopy (HRTEM), electron diffraction, energy dispersive analysis of X-rays, Fourier transform infrared, UV−vis diffuse reflectance spectroscopy, and thermal analyses. After the template extraction, the obtained mesoporous ZnS possessed a high surface area of 210 m^2/g with an average pore diameter of 28 Å. HRTEM analysis revealed a mesostructure consisting of closely spaced ZnS nanocrystallites of ∼3 nm size. The individual nanocrystallites showed typical lattice spacings corresponding to the cubic phase of ZnS. The existence of ZnS particles in a compact structure resulted in a dramatic increase in the thermal stability of the cubic phase. As revealed from optical absorption measurements, the ZnS nanoparticles exhibited quantum-size effect with a blue shift in the band gap. Finally, a systematic analysis was carried out to find the role of ultrasound on the supramolecular assembling process that leads to the generation of a mesostructure.

I. Introduction

The preparation of nanostructured materials and the fabrication of structures with ordered mesoporosity are the two foremost areas of current research in material chemistry. From the application point of view, the nanoparticles are known to possess unique chemical and electronic properties having potential usage in the fields of electronics, optics, catalysis, solar energy conversion, and magnetic materials, as well as other areas of application.[1] On the other hand, the ordered mesoporous materials, such as the M41S family of silicas and other inorganic materials, are of importance as they can find application in many diverse areas such as catalysis, adsorption, biomolecular separations, and drug delivery systems.[2] More recently, there has been a lot of interest in mesoporous and mesostructured materials in regard to electronic and optical applications, where these materials are used as hosts to align small molecules or to produce size-confined structures such as quantum dots.[3]

Combining the nanoparticles' synthesis with those leading to the templated synthesis of mesoporous materials may yield materials with novel properties and structures. Currently, this has been described as "nanotechtonics", wherein novel approaches relying on bioinspired synthesis and assembly of nano building blocks allow the design of complex architectures with controlled size, shape, orientation, and polymorphic structures.[4] In this paper, we describe a facile and versatile sonochemical route to synthesize mesoporous structures consisting of ZnS nanoparticles of a mean diameter as small as 3 nm as the building blocks.

The investigation of surfactant-mediated synthesis of chalcogenide mesostructured materials started with the work of Stupp and co-workers.[5] Since then, the approach has been extended to prepare mesostrutured materials of CdS, CdSe, ZnS, etc., with nanoparticles as the building blocks.[6] From various studies, it has been clearly shown that the specificity, stability, and degree of organization of the organic template are the crucial factors in dictating the level of control over the mesostructure of the resulting inorganic materials. However, compared to the siliceous materials, there are fewer studies on non-siliceous materials producing mesostructures owing to the complexity in the chemical behavior of non-siliceous materials, which often makes them more susceptible to hydrolysis, redox reactions, or phase transitions accompanied by thermal breakdown of the mesostructure.[7] More importantly, for these materials removal of the template had been difficult,

* To whom correspondence may be addressed: fax, +972-3-5351250; tel, +972-3-5318315. e-mail, gedanken@mail.biu.ac.il.
[†] Bar-Ilan University.
[‡] The Chinese University of Hong Kong.
[§] Max Planck Institute of Colloids and Interfaces.

(1) (a) Rao, C. N. R.; Cheetham, A. K. *J. Mater. Chem.* **2001**, *11*, 2887. (b) Trindade, T.; O'Brien, P.; Pickett, N. L. *Chem. Mater.* **2001**, *13*, 3843.
(2) (a) Beck, J. S.; Vartuli, J. C.; Roth, W. J.; Leonowicz, M. E.; Kresge, C. T.; Schmitt, K. D.; Chu, C. T. W.; Olson, D. H.; Sheppard, E. W.; Mccullen, S. B.; Higgins, J. B.; Schlenker, J. L. *J. Am. Chem. Soc.* **1992**, *114*, 10834. (b) He, X.; Antonelli, D. *Angew. Chem., Int. Ed.* **2001**, *41*, 214. (c) Ozin, G. A. *Chem. Commun.* **2000**, 419.
(3) Scott, B. J.; Wirnsberger, G.; Stucky, G. D. *Chem. Mater.* **2001**, *13*, 3140.
(4) Davis, S. A.; Breulmann, M.; Rhodes, K. H.; Zhang, B.; Mann, S. *Chem. Mater.* **2001**, *13*, 3218.
(5) (a) Braun, P. V.; Osenar, P.; Stupp, S. I. *Nature* **1996**, *380*, 325. (b) Osenar, P.; Braun, P. V.; Stupp, S. I. *Adv. Mater.* **1996**, *8*, 1022. (c) Braun, P. V.; Osenar, P.; Tohver, V.; Kennedy, S. B.; Stupp, S. I. *J. Am. Chem. Soc.* **1999**, *121*, 7302.
(6) (a) MacLachlan, M. J.; Coombs, N.; Bedard, R. L.; White, S.; Thompson, L. K.; Ozin, G. A. *J. Am. Chem. Soc.* **1999**, *121*, 12005. (b) Wachhold, M.; Rangan, K. K.; Billinge, S. J. L.; Petkov, V.; Heising, J.; Kanatzidis, M. G. *Adv. Mater.* **2000**, *12*, 85. (c) Rangan, K. K.; Trikalitis, P. N.; Kanatzidis, M. G. *J. Am. Chem. Soc.* **2000**, *122*, 10230. (d) Li, J. Q.; Kessler, H. *Micro. Mater.* **1997**, *9*, 141. (e) Trikalitis, P. N.; Rangan, K. K.; Bakas, T.; Kanatzidis, M. G. *Nature* **2001**, *410*, 671. (f) Li, J. Q.; Kessler, H.; Soulard, M.; Khouchaf, L.; Tuilier, M. H. *Adv. Mater.* **1998**, *10*, 946.
(7) Schuth, F. *Chem. Mater.* **2001**, *13*, 3184.

10.1021/la0343627 CCC: $25.00
Published on Web 06/11/2003

and thus, no mesoporous materials, but only mesostructured materials, could be obtained.[7] As far as the nanoparticle assembly is concerned, obtaining a porous structure was not easy mainly because the constituent nanoparticles are weakly bound to each other, and thus the structure collapses upon removal of the template. Our results show for the first time that a sonochemical method can be used to assemble ZnS nanoparticles on an organic template in such a way that a stable mesoporous framework is produced even after removal of the template.

Mesoporous ZnS was synthesized by a neutral templating route to assemble the ZnS nanoparticles that are generated in situ by the well-known ultrasound-mediated nanostructure fabrication method. The sonochemical effect is based on acoustic cavitation, a phenomenon which results from the continuous formation, growth, and implosive collapse of bubbles within a liquid, generating local hot spots of high temperature and pressure.[8] Nanostructured metals, alloys, oxides, carbides, and sulfides can all be prepared by this general route and have been studied extensively by our group and others.[9] Recently, we have shown that the effect of ultrasound can also be used in fabricating various mesoporous inorganic materials possessing a high surface area.[10] It has been proposed that the ultrasound-generated high temperature near the liquid−air interface accelerates the polymerization of the inorganic moieties attached to the micelles, resulting in a shorter preparation time. In this article, we describe a unique combination of the above two methodologies comprising the nanoparticle synthesis and supramolecular assembly under the influence of ultrasound.

II. Experimental Section

A. Synthesis. Mesostructured ZnS particles were synthesized by an ultrasound-mediated process using dodecylamine (DDA) and thioacetamide (TAA) as the templating and sulfiding agents, respectively. The reaction mixture was prepared in the following molar ratios: 0.4−0.6 DDA:1.0 $Zn(Ac)_2$:1.0 TAA:600 H_2O. In a typical experiment, 0.0033 mol of DDA was dissolved in 10 mL of ethanol and to this a solution of zinc acetate dihydrate (0.0055 mol) and thioacetamide (0.0055 mol) in 60 mL of doubly distilled water was added. The resulting solution was sonicated with a high-intensity ultrasound horn (Sonics and Materials, VC-600, Ti horn, 20 kHz, operated at 60% of the 100 W cm^{-2} power). A white precipitate gradually appeared, and the sonication was continued for 3 h, during which time the temperature rose to 80 °C. The resulting precipitate was centrifuged, washed several times with water and ethanol, and then vacuum-dried. The organic template was removed from the as-synthesized material by treating the powder in hot ethanol (60 °C) for 24 h with continuous stirring. Increase in the treatment duration more than 24 h up to 48 h did not improve the result with any further removal of the organic template.

B. Characterization. The X-ray diffraction patterns of the products were recorded using a Bruker AXS D8 Advance Powder X-ray diffractometer (using Cu Kα $\lambda = 1.5418$ Å radiation). Low-resolution TEM images were obtained with a JEOL-JSM-840 electron microscope operated at 100 kV. High-resolution transmission electron microscopy (HRTEM) micrographs were obtained with a Zeiss EM 912 OMEGA operating at an acceleration voltage of 120 kV. Scanning electron microscope (SEM) images were recorded on a LEO-1550 (field emission microscope, GEMINI). The thermogravimetric analysis (TGA) and differential scanning calorimetry (DSC) measurements were carried out under nitrogen on Mettler Toledo TGA/SDTA 851 and DSC-301 instruments, respectively. To check the thermal stability of the template-extracted ZnS sample, the materials were collected after heating the sample up to 600 and 1000 °C in separate TGA experiments and further analyzed. N_2 adsorption−desorption isotherms were collected on a Micromeritics 2010 adsorption analyzer at 77 K. Fourier transform infrared (FT-IR) spectroscopy was carried out on a Nicolet Impact 410 FTIR spectrometer. UV−vis diffuse reflectance spectra were collected from a Varian Cary 100 instrument as plots of Kubelka−Munk correction function.

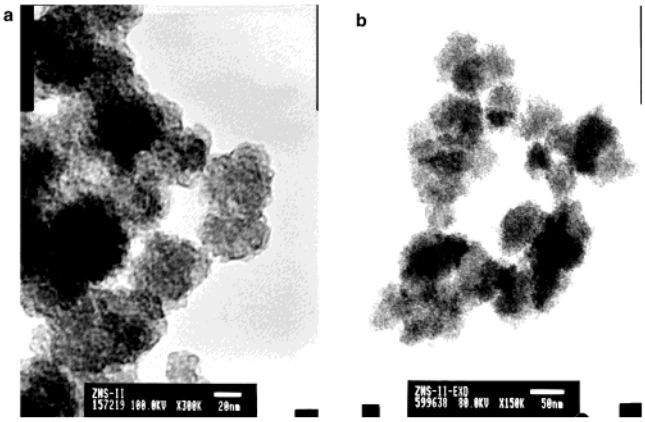

Figure 1. Low-resolution TEM images of the (a) as-synthesized and (b) template-extracted ZnS samples depicting the morphology.

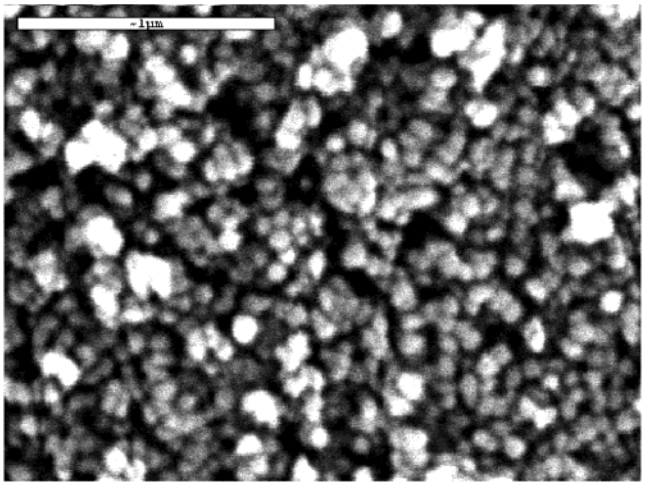

Figure 2. SEM image of the mesoporous ZnS sample after the template extraction.

III. Results and Discussion

A. Morphology. The morphological characteristics of the obtained products were analyzed by transmission electron microscopy (TEM). The TEM images of the as-synthesized and extracted samples are shown in Figure 1. Small aggregates of nanoparticles were seen from the TEM images. The size of these aggregates varied from 50 to100 nm having a nearly spherical morphology. It was previously observed that the overall morphology of the product strongly depends on the amount of the organic template and the inorganic precursor present in the solution.[10] In the present case, aggregates of nearly

(8) (a) Suslick, K. S.; Price, G. *Annu. Rev. Mater. Sci.* **1999**, *29*, 295. (b) Suslick, K. S. *Science* **1990**, *247*, 1439. (c) Suslick, K. S.; Choe, S. B.; Cichowlas, A. A.; Grinstaff, M. W. *Nature* **1991**, *353*, 414.

(9) (a) Nikitenko, S. I.; Koltypin, Y.; Palchik, O.; Felner, I.; Xu, X. N.; Gedanken, A. *Angew. Chem., Int. Ed.* **2001**, *40*, 4447. (b) Avivi, S.; Mastai, Y.; Gedanken, A. *J. Am. Chem. Soc.* **2000**, *122*, 4331. (c) Mastai, Y.; Homyonfer, M.; Gedanken, A.; Hodes, G. *Adv. Mater.* **1999**, *11*, 1010. (d) Prozorov, T.; Gedanken, A. *Adv. Mater.* **1998**, *10*, 532.

(10) (a) Gedanken, A.; Tang, X. H.; Wang, Y. Q.; Perkas, N.; Koltypin, Y.; Landau, M. V.; Vradman, L.; Herskowitz, M. *Chem.-Eur. J.* **2001**, *7*, 4546. (b) Rana, R. K.; Mastai, Y.; Gedanken, A. *Adv. Mater.* **2002**, *14*, 1414. (c) Tang, X. H.; Liu, S. W.; Wang, Y. Q.; Huang, W. P.; Sominski, E.; Palchik, O.; Koltypin, Y.; Gedanken, A. *J. Chem. Soc, Chem. Commun.* **2000**, 2119. (d) Wang, Y. Q.; Tang, X. H.; Yin, L. X.; Huang, W. P.; Hacohen, Y. R.; Gedanken, A. *Adv. Mater.* **2000**, *12*, 1183.

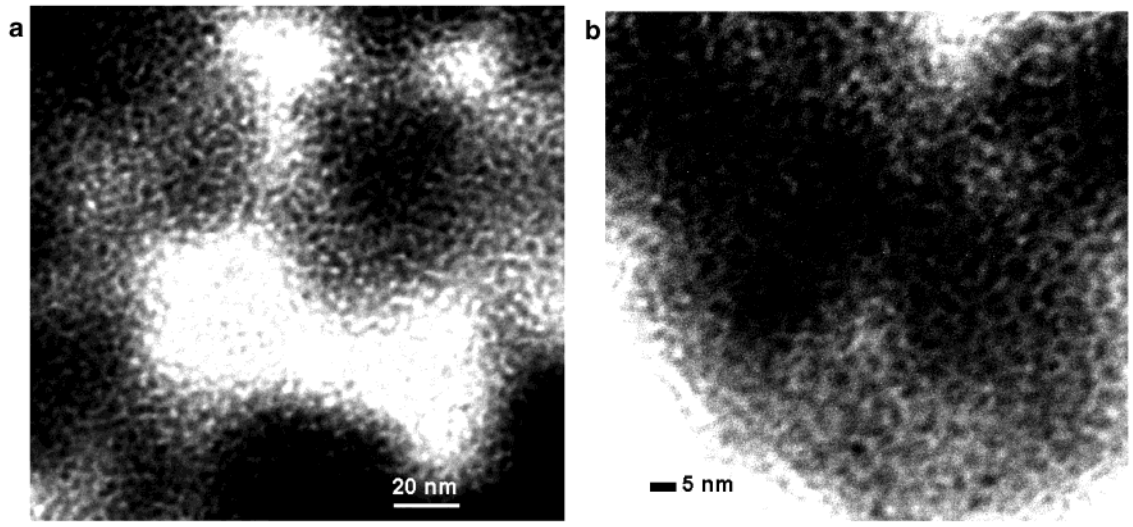

Figure 3. HRTEM of the (a) as-synthesized and (b) template-extracted ZnS sample depicting the mesoporous structure.

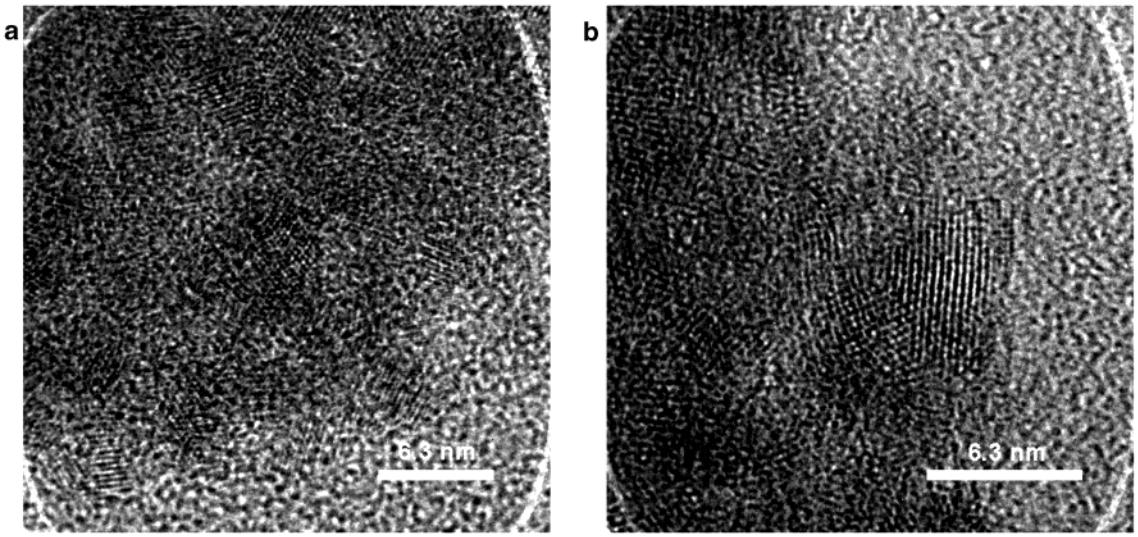

Figure 4. HRTEM images of ZnS (a) as-synthesized and (b) extracted samples depicting the lattice fringes of individual nanocrystallites.

spherical morphology were obtained when the amine-to-zinc molar ratio was restricted within 0.4−0.6 for an amine concentration of 0.05 mol/L. The three-dimensional structure of the aggregates was evident from the scanning electron microscopic image shown in Figure 2.

HRTEM images of the samples are shown in Figure 3. Within each aggregate, the pore openings surrounded by the nanoparticles were clearly visible. The nanoparticles were of 2−4 nm average diameter. There were no obvious morphological changes after the template was removed, indicating that the porous structure of the ZnS sample was stable and unaffected by the template-extraction method. To characterize the nanostructures, atomically resolved HRTEM analysis was carried out. The images of the individual nanocrystallites depict the well-resolved lattice planes as illustrated in Figure 4. Careful observation of these planes showed two sets of spacings, one having a *d* spacing of ∼2.6 Å and the other having 3 Å. These spacings typically correspond to (200) and (111) planes of the cubic ZnS phase, respectively. The close proximity of the nanocrystallites seen in the images suggested a compact arrangement of the individual crystallites. It was also clear from the images that the nanocrystals are arranged surrounding an empty space. The empty space represents the pore openings, the estimated size of which varied from 26 to 30 Å.

B. Structural Analysis. Structural information of the nanocrystallites was obtained from selected area electron diffraction analyses. A typical selected area electron diffraction pattern obtained from the extracted sample is shown in Figure 5. As expected, the electron diffraction (ED) pattern shows a set of rings due to the random orientation of the crystallites, corresponding to diffraction from different planes of the nanocrystallites. The well-resolved three rings could be assigned to (111), (220), and (311) planes of the cubic ZnS phase. The energy dispersive analysis of X-rays (EDAX) of the sample showed a stoichiometric ratio for Zn and S within an accuracy of ±2%. The ratio remained unchanged after the template extraction.

The ZnS sample exhibited a low-angle X-ray diffraction (XRD) peak before and after the template removal. As shown in Figure 6, the peaks were broad and there were no higher order peaks that indicated a defectively ordered pore structure. A single intense XRD peak at high *d* spacing generally corresponds to a randomly ordered supramolecular-templated inorganic structure.[11] The single

(11) Tanev, P. T.; Pinnavaia, T. J. *Science* **1995**, *267*, 865.

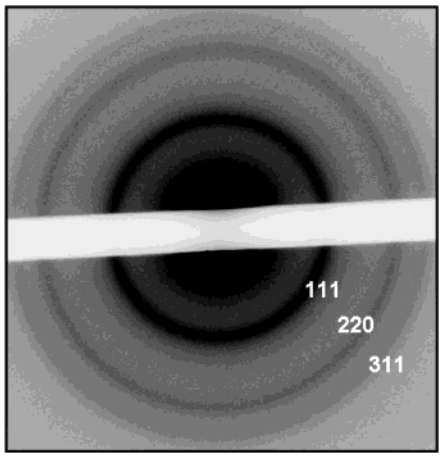

Figure 5. Electron diffraction pattern from the template-extracted ZnS sample.

peak represents an average distance between the inorganic walls, which can be calculated from Bragg's law. For the as-prepared and template-extracted samples, the Bragg spacing was about 6.8 and 5.3 nm, respectively. The shift in the diffraction peak is presumably due to shrinkage in the pore sizes after the template removal. Nevertheless, the presence of the peak is indicative of an intact porous structure of the template-extracted sample.

The wide-angle XRD patterns of the samples are shown in Figure 6. In both cases, three broad peaks were observed, which could be indexed to a cubic ZnS structure. From the full width at half-maximum of the (111) diffraction peak, the average size of the crystallites was estimated using Scherrer's formula. In the as-synthesized sample the average crystallite size was 2.6−2.7 nm, and it remained the same after template extraction. The calculated particle size matched well with the size determined from the HRTEM images.

C. N_2-Sorption Studies. Typical nitrogen adsorption−desorption isotherms at 77 K for the template-extracted materials and the corresponding pore size distribution are shown in Figure 7. The resulting isotherm could be identified as a type IV isotherm. A small hysteresis in the isotherm shows that the pores are accessible by the gas molecules without much hindrance. The increase in the nitrogen uptake at relative pressures in the range between p/p_0 0.42 and 0.6 was reflected in a wide pore size distribution. As calculated by the Bopp−Jancso−Heinzinger method, the average pore diameter was 28 Å (inset, Figure 7), in good agreement with the HRTEM results. Subtracting the pore size from the interplanar distance, we obtained a pore-wall thickness of ∼2.5 nm. The pore-wall thickness roughly corresponds to the size of one ZnS nanocrystallite. The Brunauer−Emmett−Teller (BET) surface area of the sample was 210 m^2/g, whereas the as-synthesized material had a surface area of 10 m^2/g. Clearly, the increase in surface area after the template extraction could be attributed to the mesopores present in the structure. On the other hand, for ZnS nanoparticles that were synthesized sonochemically in the absence of any surfactant molecules, the BET surface area was only 15 m^2/g. Such a low value of surface area is indicative of a highly agglomerated structure.

D. FT-IR Analysis. FT-IR spectra of various samples are shown in Figure 8. The IR spectra of the as-synthesized ZnS provided evidence for the presence of an organic template, which gives the typical absorbances at 2920 and 2850 cm^{-1} due to the aliphatic C−H vibrations. For the template-extracted sample, the corresponding band

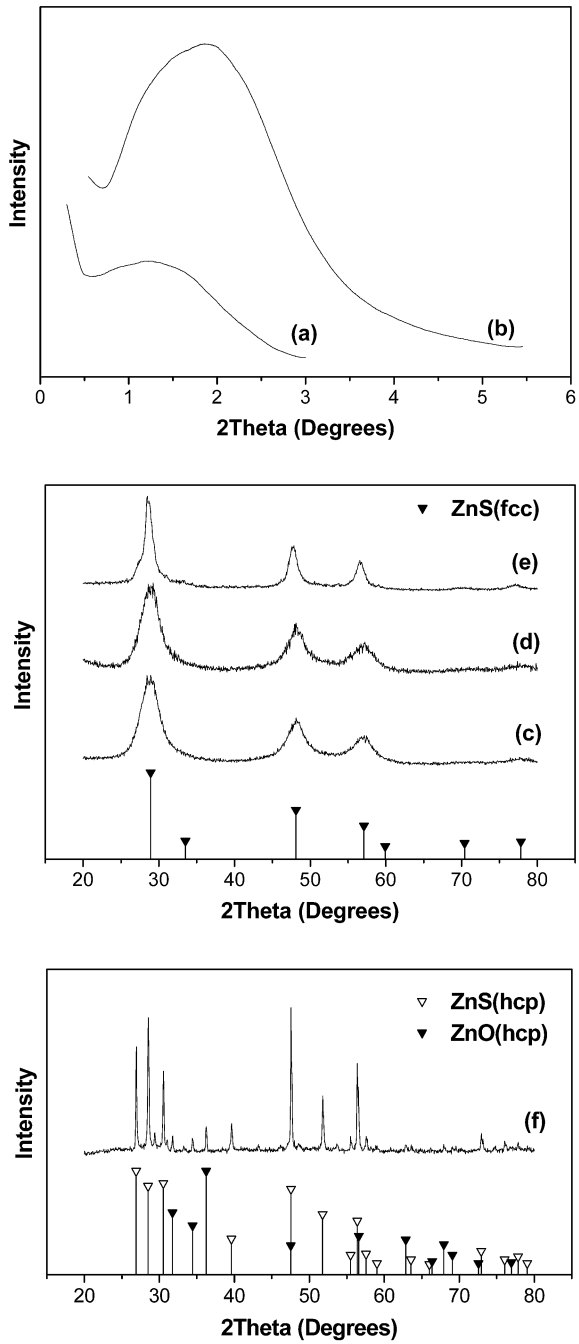

Figure 6. Low-angle XRD of (a) the as-synthesized and (b) the template-extracted ZnS samples; wide-angle XRD of (c) the as-synthesized and (d) the template-extracted ZnS samples; (e) the template-extracted ZnS sample heated to 600 °C and (f) 1000 °C under a nitrogen atmosphere. (The line spectra represent the standard XRD peak intensities from JSPDS files: ZnS 88−20, ZnS 36−1450, and ZnO 79−2205.)

intensities drastically reduced, implying an efficient removal of most of the organic molecules. To compare the results, IR spectrum of the zinc oxide[12] has also been included in Figure 8. The zinc oxide showed a strong absorption at 430 cm^{-1}, corresponding to the Zn−O stretching vibrations.[13] On the other hand, the ZnS samples did not show any IR absorption in this region.

(12) The ZnO was prepared by sonicating an aqueous solution of zinc acetate (600 mg) and dodecylamine (100 mg) under similar sonochemical conditions employed for mesoporous ZnS synthesis.

(13) Trindade, T.; Pedrosa de Jesus, J. D.; O'Brien, P. *J. Mater. Chem.* **1994**, *4*, 1611.

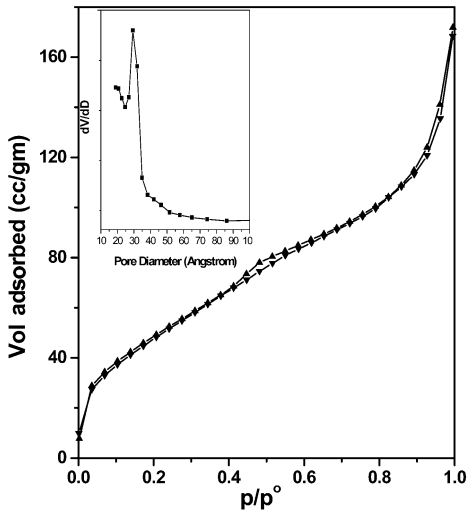

Figure 7. N_2-adsorption−desorption isotherms for the template-extracted ZnS sample and (inset) the corresponding pore-size distribution curve.

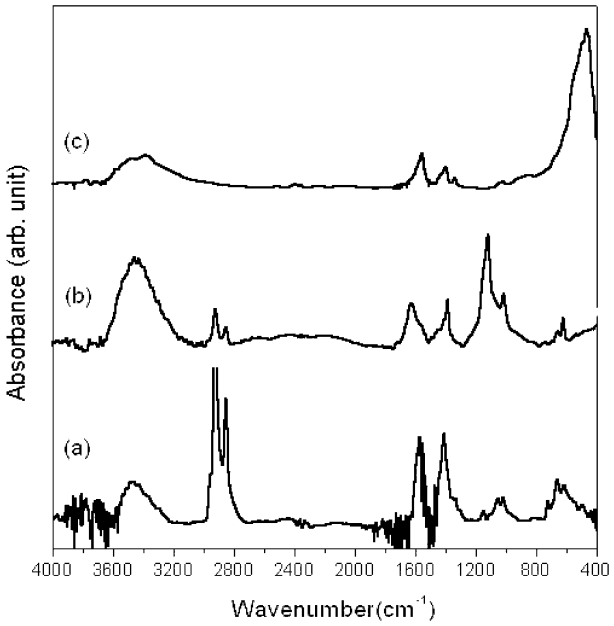

Figure 8. FT-IR spectra of (a) as-synthesized mesostructured ZnS, (b) template-extracted mesoporous ZnS, and (c) as-synthesized ZnO.

Thus, any possible contamination of the sample with zinc oxide was ruled out.

However, it was earlier reported that the ZnS films prepared from an alkaline ammonia solution of a zinc salt and thioacetamide/thiourea generally contained a significant amount of oxygen.[14] From extended X-ray absorption fine structure (EXAFS) studies, Mokili et al. confirmed the presence of oxygen in the form of hydroxides.[15] The presence of hydroxides could be seen in the IR spectra of ZnS samples (Figure 8) having absorbance bands around 1115 cm^{-1}.[16] It was also previously pointed out that many of the films reported as ZnS, which had not been rigorously characterized, were probably at best contaminated with zinc oxide or hydroxide.[17] In our case the presence of oxygen was confirmed from EDAX analysis, and the amount was found to increase after the template extraction. A corresponding increase in the IR band intensities in the 1100−625 cm^{-1} and 3300−3500 cm^{-1} regions could also be seen in the spectrum of the template-extracted ZnS sample. This suggests that the hydroxides are mostly present as surface species occupying the positions to which template molecules were previously attached.

E. Thermal Analysis. The thermal stability of the materials was investigated by TGA. As shown in Figure 9, the TGA showed two distinct weight losses arising from the desorption of water (below 150 °C) and the decomposition of the organic template (250−500 °C). The total amount of the organic template present in the sample was 20 wt %. After 500 °C there was no weight loss until 800 °C. While bulk ZnS undergoes a phase transition from zinc blend to its wurtzite structure at 1050 °C, free-standing nanocrystals of ZnS were previously observed to undergo the same transition at temperatures as low as 500 °C.[18] The lowering in the transition temperature was attributed to the change of surface energy accompanied with an increase in the crystallite size during the annealing process of the nanocrystals. In contrast, in our case, the XRD pattern for the mesostructured ZnS sample that was heated to 600 °C differed little from those obtained for the as-synthesized sample, except for a narrowing down of the XRD peaks (Figure 6). This implied a better thermal stability for the cubic phase of ZnS nanoparticles that were mesostructurally arranged to form a superstructure. Clearly, these self-assembled ZnS nanoparticles were quite different from the bulk material as well as the free-standing nanocrystals. A similar phenomenon was previously observed by Breen et al. for ZnS nanoparticles coated on polystyrene microspheres.[19] When the mesostrucured ZnS sample was heated to 1000 °C, it changed to a ZnS wurtzite structure and partly oxidized to give zinc oxide (Figure 6).

As far as the structure of ZnS is concerned, the zinc blende and wurtzite structures are very similar and can both be regarded as networks of ZnS_4 tetrahedra.[20] In zinc blende, layers of tetrahedral form an ABC stacking sequence and orientation of all the tetrahedral is identical. In wurtzite, however, the layers form an AB sequence and alternate layers are rotated by 180° about the *c* axis. A phase transition from cubic to hexagonal can thus proceed by creation of stacking faults, which can be considered as thin layers of wurtzite structure introduced in the blende structure.[21] Two or more such stacking faults then form nanodomain of wurtzite structure. This, however, requires a creation and glide of partial dislocations in order to create stacking faults and which, in our case, was probably hindered by the closely packed nanocrystallites. It had also been reported that the surface modification of ZnS nanocrystals by binding thiolate and carboxylate ions to the surface zinc atoms could alter the surface energy of the crystals.[22] This change in surface energy could then stabilize the cubic or hexagonal phase, depending upon the chemical species attached onto the

(14) Mokili, B.; Froment, M.; Lincot, D. *J. Phys. Fr. IV* **1995**, *5*, C3−261.
(15) Mokili, B.; Charreire, Y.; Cortes, R.; Lincot, D. *Thin Solid Films* **1996**, *288*, 21.
(16) Srivastava, O. K.; Secco, E. A. *Can. J. Chem.* **1967**, *45*, 585.
(17) O'Brien, P.; McAleese, J. *J. Mater Chem.* **1998**, *8*, 2309.
(18) Qadri, S.; Skelton, E. F.; Hsu, D.; Dinsmore, A. D.; Yang, J.; Gray, H. F.; Ratna, B. R. *Phys. Rev., B: Condens. Matter.* **1999**, *60*, 9191.
(19) Breen, M. L.; Dinsmore, A. D.; Pink, R. H.; Qadri, S. B.; Ratna, B. R.; *Langmuir* **2001**, *17*, 903.
(20) West, A. R. *Solid State Chemistry and Its Applications*; John Wiley & Sons: Chichester, U.K., 1984.
(21) Ricolleau, C.; Audinet, L.; Gandais, M.; Gacoin, T. *Eur. Phys. J. D* **1999**, *9*, 565.
(22) Murakoshi, K.; Hosokawa, H.; Tanaka, N.; Saito, M.; Wada, Y.; Sakata, T.; Mori H.; Yanagida, S. *J. Chem. Soc, Chem. Commun.* **1998**, 321.

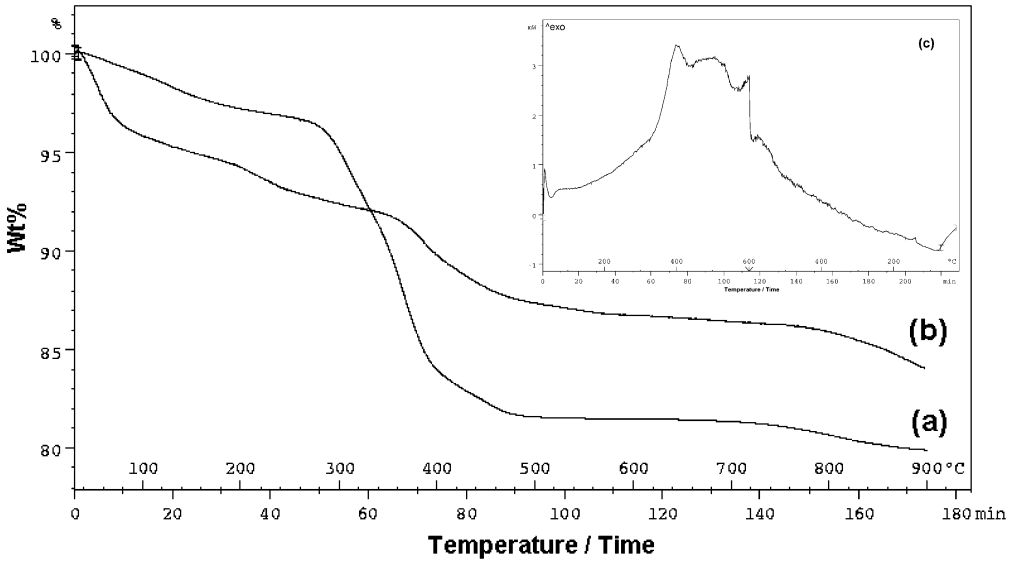

Figure 9. (a) TGA curve for the as-synthesized mesostructured ZnS sample. (b and c) TGA and DSC curves for the template-extracted mesoporous ZnS sample, respectively.

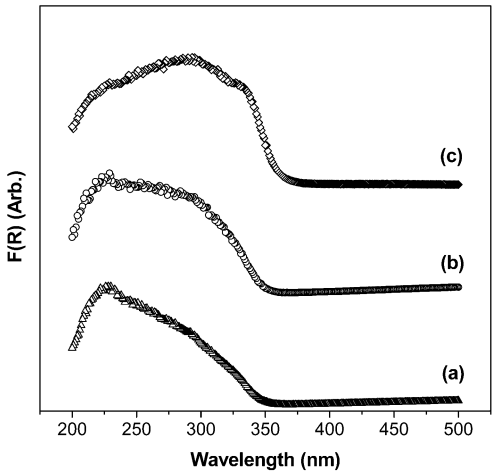

Figure 10. Diffuse reflectance UV−vis spectra of (a) the as-synthesized mesostructured ZnS sample, (b) the template-extracted mesoporous ZnS, and (c) Zn.

surface. So the better stability of the cubic phase may be due to a compact arrangement of the nanocrystallites and/or the surface-bound dodecylamine molecules present in the mesostructure.

The TGA of the extracted sample is shown in Figure 9b. The weight loss of ∼5% in the temperature region 360−500 °C was due to the decomposition of the remaining surfactant molecules after extraction. The corresponding DSC profile for the extracted sample showed an exothermic peak at 400 °C due to the decomposition of the remaining surfactants. The high onset decomposition temperature indicated that the surfactant molecules were more strongly attached to the inorganic framework, and thus it was difficult to remove the surfactants completely by the solvent extraction method. It is believed that the remaining surfactant molecules form a thin layer between the nanoparticles to keep the mesoporous structure intact even after removal of the template. Thus, the stability of the structure was attributed to two factors, i.e., the closeness of the nanoparticles and the presence of a low amount of surfactant presumably acting as a binder.

F. Optical Properties. UV−vis diffuse reflectance studies were performed to characterize the optical properties of the ZnS samples. As shown in Figure 10, both the as-prepared and template-extracted samples showed an onset of absorption at 350 nm. The sharp absorption edges for the samples indicate that the synthesized particles have a relatively narrow size distribution. In comparison with the band gap for the bulk ZnS, the absorption edges were found to be blue shifted by 60 nm. Such a shift in the optical absorption spectrum is known to take place because of the quantum confinement effect, which occurs in the case of nanoparticles when the particle size becomes comparable with or smaller than the Bohr radius of exciton. The ZnS nanocrystallites synthesized in the present study had sizes less than the Bohr excitonic diameter of ZnS, which is around 5.5 nm.[23]

It should be noted that the organic component present in the sample may interact with ZnS, and as a consequence it may pose an effect on the optical properties. Zhang et al. reported a strong host−guest effect of the surfactant molecules on the ZnS particles confined in MCM-41 channels, thus inducing a change in the spectrum shape. A similar change in shape could be seen for the mesoporous ZnS samples when compared with the spectrum of ZnS nanoparticles, which were prepared sonochemically in the absence of any structure-directing agent.[24]

G. Mechanism. The mechanism of ZnS nanoparticle formation under the influence of ultrasound has been reported elsewhere.[25] The proposed reactions occurring during sonication that leads to ZnS formation are given in eqs 1−3. Equation 1 represents the formation of primary radicals from the ultrasound-initiated dissociation of water. The main reactions leading to the formation of ZnS nanoclusters are given in eqs 2 and 3. The formation of H_2S via reaction 2, which has previously been suggested,[26] further reacts with $Zn(Ac)_2$ to yield ZnS. In the present case, the freshly generated ZnS nanoclusters interact with the dodecylamine (DDA) surfactants and assemble to form a ZnS−DDA mesostructure composite.

(23) (a) Yoffe, A. D. *Adv. Phys.* **1993**, *42*, 173. (b) Kayanuma, Y. *Phys. Rev. B* **1988**, *38*, 9797.
(24) Zhang, W.-H.; Shi, J.-L.; Chen, H.-R.; Hua, Z.-L.; Yan, D.-S. *Chem. Mater.* **2001**, *13*, 648.
(25) Dhas, N. A.; Zaban, A.; Gedanken, A. *Chem. Mater.* **1999**, *11*, 806.
(26) (a) Nicolau, Y. F.; Menard, J. C. *J. Colloid Interface Sci.* **1992**, *148*, 551. (b) Wilhelmy, D. M.; Matijevic, E. *J. Chem. Soc., Faraday Trans. 1* **1984**, *80*, 563.

As the surfactant molecules have the ability to accumulate at the air/liquid interface surrounding the bubbles, it is highly plausible that a self-assembling process can take place in the interfacial region between the cavitating bubbles and the bulk solution. Although the temperature in the interfacial region is lower than in the gas-phase inner region of the bubble, it is still high enough to induce a sonochemical reaction.

$$H_2O \xrightarrow{)))} H^\bullet + OH^\bullet \quad (1)$$

$$2H^\bullet + RS^\bullet \xrightarrow{)))} H_2S + R^\bullet \quad (RS = \text{thioacetamide}) \quad (2)$$

$$H_2S + Zn(Ac)_2 \rightarrow ZnS + 2AcH \quad (3)$$

Recently, Yamaguchi et al. reported on a detailed study on the reaction mechanism involved in the chemical bath deposition of ZnS thin films from an aqueous solution of zinc acetate and thioacetamide (TAA).[27] They proposed a model according to which zinc ion initially forms a complex with TAA molecules. The decomposition of the complex leads to the formation of ZnS molecules, which then gather to form ZnS nuclei. The rate-limiting step was related to the formation of individual molecules of ZnS, and the individual nature of these reacting species was found responsible for the single crystalline nature of the ZnS nanocrystallites with invariable size.[27] This hypothesis of nucleation-controlled growth is in good agreement with our results, where the nanocrystallites are of ~3 nm sizes. Normally, nanocrystallites of these dimensions have a greater tendency to agglomerate, thus forming bigger particles. In the present study, we have chosen a system in which these nanocrystallites are prevented from random agglomeration by the presence of an organic template under sonochemical conditions. The particle agglomeration is generally governed by the surface charge of the particles. The isoelectric point for spherical ZnS colloids has been reported as either pH 2.3 or 3.[28] Thus, in our experimental condition (pH = 6−7) the ZnS particles should be negatively charged. However, it has also been reported that the isoelectric point of ZnS colloids is affected not only by the pH but also by coexisting Zn^{2+} and $Zn(OH)^{2+}$ ions. The presence of these cations generally shifts the surface charge positively. In our case, the fact that a mesoporous structure is created indicates that the individual ZnS nanocrystallites have the ability to attach themselves to the DDA molecules, thus preventing the random agglomeration of the particles. Once the nanocrystallites are bound to the DDA molecules, they rearrange themselves in an ordered fashion to form the mesostructured pattern at the air−water interface region of the cavitating bubbles.

To gain more knowledge about the self-assembly process, we carried out a control experiment, where sonication of an aqueous solution of zinc acetate and dodecylamine, without the presence of any sulfur source, was performed under similar sonochemical conditions.[12] The sonication produced ZnO particles with high crystallinity, as evident from the XRD pattern shown in Figure 11. The particles were shaped like hexagons and cubes of sizes >100 nm. However, no superstructure was observed consisting of zinc oxide and dodecylamine. As seen in the IR spectrum (Figure 8), the zinc oxide did not show any evidence of the template being attached to the inorganic matrix. It further supported the above observation indicating that there was no templating effect of the amine on ZnO formation. Moreover, the sizes of the zinc oxide particles were big enough (>100 nm) to be assembled around the micelles. However, in the case of ZnS, the formation of a mesoporous structure was the result of the generation of zinc sulfide nanoparticles of very small sizes (~3 nm), which could assemble themselves around the template.

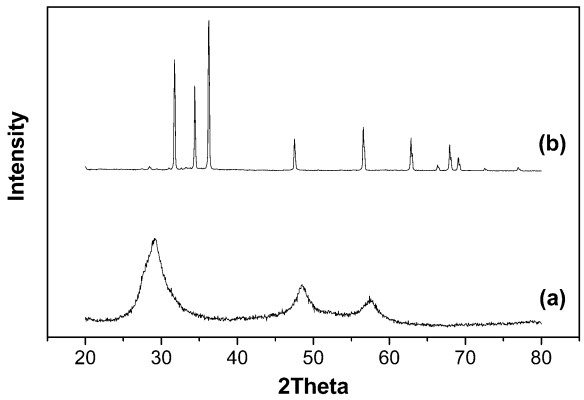

Figure 11. Wide-angle XRD of the (a) ZnS nanoparticles obtained in the absence of the template and (b) ZnO particles obtained in the absence of thioacetamide (the synthesis conditions for both the samples were kept same as that for the synthesis of mesostructured ZnS except that for the first case dodecylamine and for the second case thioacetamide was not used in the reaction mixture, respectively).

In the case where the fabrication of a mesostructure requires nanoparticles as the building blocks, a preformed sample of ZnS nanoparticles should be sufficient to be used directly as the precursor for the formation of mesostructured material. To verify this, we did another experiment where the ZnS nanoparticles were first generated by the known ultrasound method. The sample exhibited a similar XRD pattern (Figure 11), as observed for the meostructured ZnS samples. These nanoparticles were then mixed with a dodecylamine solution and sonicated under similar conditions. The resulting material was found to be non-mesostructured. As revealed from the TEM analysis, the reason for not forming a superstructure might be because of the already agglomerated form of the preformed ZnS nanoparticles, which could not be rearranged by the template molecules. This leads to the conclusion that the in situ generation of ZnS nanoparticles and the size of the particles are the crucial factors for fabricating a mesostructured material that is composed of nanoparticles as building blocks.

IV. Conclusions

In conclusion, the results illustrate that the sonochemical method provides a facile and efficient route to specifically prepare non-siliceous mesoporous materials where the nanoparticles are generated in situ by the well-known ultrasound-mediated technique. The cavitational effect of the ultrasound eventually generates a compact mesostructure consisting of nanoparticles and surfactants. The structure remains stable even after removal of the surfactant creating a porous structure with a high surface area and a better thermal stability for the cubic ZnS nanocrystallites. Moreover, the approach does not require any specialized structure-directing reagents other than the normally used amines. The simultaneous use of ultrasound-induced cavitation to generate semiconductor nanoparticles and supramolecular templating may be

(27) Yamaguchi, K.; Yoshida, T.; Lincot, D.; Minoura, H. *J. Phys. Chem. B* **2002**, *ASAP*, Dec. 3.
(28) Sostaric, J. Z.; Caruso-Hubson, R. A.; Mulvaney, P.; Grieser, F. *J. Chem. Soc., Faraday Trans.* **1997**, *93*, 1791.

applicable in the synthesis of a wide variety of technologically important materials with well-defined and stable porosity.

Acknowledgment. We thank the Israeli Ministry of Science, Culture and Sports for supporting this research via an Infrastructure grant. R.K.R. thanks the Bar-Ilan Research Authority for his postdoctoral fellowship. A.G. thanks the BMBF, Germany for partial support of this research via a DIP grant (Deutsche−Israeli projects).

LA0343627